Available online at www.sciencedirect.com
ScienceDirect
Journal of Magnetic Resonance 183 (2006) 228–234
JMR Journal of Magnetic Resonance
www.elsevier.com/locate/jmr

A constant gradient unilateral magnet for near-surface MRI profiling

Andrew E. Marble [a,b], Igor V. Mastikhin [a,*], Bruce G. Colpitts [b], Bruce J. Balcom [a]

[a] MRI Centre, Department of Physics, P.O. Box 4400, University of New Brunswick, Fredericton, New Brunswick, Canada E3B 5A3
[b] Department of Electrical and Computer Engineering, P.O. Box 4400, University of New Brunswick, Fredericton, New Brunswick, Canada E3B 5A3

Received 19 July 2006; revised 29 August 2006
Available online 25 September 2006

Abstract

The design and construction of a unilateral NMR (UMR) magnet assembly for near-surface 1D profiling is presented. The arrangement consists of a single permanent magnet topped with a shaped iron pole cap. The analytically determined profile of the pole cap shapes the field over the magnet, giving a constant gradient of 31 G/cm over a 8 mm depth at a ^{1}H frequency of 4.26 MHz in a spot ~5 mm wide. The moderate gradient allows 1D profiling of planar samples with a frequency encoded spin-echo experiment. The curvature of the magnetic field limits the available resolution to 100's of μm. The device is suitable for profiling planar samples in which a coarse resolution but large spatial extent is desired.

Keywords: Unilateral magnetic resonance; Inhomogeneous fields; Magnet design; Profiling

1. Introduction

Single-sided or unilateral nuclear magnetic resonance (UMR) uses an open configuration of magnets to produce a MR compatible magnetic field in a remote sensitive volume [1–4]. Although, the field within this volume is necessarily inhomogeneous, UMR sensors have been widely employed for bulk MR measurements. This allows parameters such as T_2, T_1, and self diffusion coefficients to be obtained from arbitrarily sized samples, and has found diverse uses such as down-hole oil well logging [1], and characterization of food products [5].

By controlling the inhomogeneity of the field, UMR has been extended to imaging applications by various groups. Prado [6] describes a single-sided imaging sensor employing a specially designed magnet array producing a flat sensitive volume. Using a computer controlled capacitor switching scheme, the resonant frequency of a surface coil was varied between 14 and 6 MHz to select planes in the inhomogeneous field. The field gradient over the sensitive volume varied from −1400 to −260 G/cm. Perlo et al. [7] extend this idea, using a sensor with a flat sensitive volume augmented with gradient coils, to give 2D spatial resolution in a flat slice, the depth of which can be adjusted through manual tuning. In both cases, the depth resolution is difficult to control. The operating frequency must be retuned for each depth, and the volume excited is dependent on the pulse bandwidth. Furthermore, the strong variation in field strength with depth can cause difficulties in image contrast in samples with field-dependent relaxation times.

To overcome this difficulty, Perlo et al. [8] developed a sensor with a thin, flat spot at a single, narrow frequency band. By moving the sensor relative to the sample using a manually controlled lift, one-dimensional profiles with a resolution below 10 μm were possible. Using a different approach, Rahmatallah et al. [9] employed the field of a magnetized cylinder [10] which produces a point where the second spatial derivative of the field vanishes in the depth direction, giving an approximately constant B_0 gradient of −570 G/cm at 10.9 MHz. Profiles with a resolution of about 60 μm over a ~1 mm depth were reported, with the resolution being limited by the flatness of the sensitive volume. Profiling measurements with a similar resolution and depth range using the stray field from the end of a Halbach magnet have also been recently reported [11].

* Corresponding author. Fax: +1 506 453 4581.
E-mail address: mast@unb.ca (I.V. Mastikhin).

1090-7807/$ - see front matter
doi:10.1016/j.jmr.2006.08.013

Brown et al. [12] used a NMR-MOUSE [3] like magnet in conjunction with an electromagnet to oppose the magnetic field produced by the permanent magnets. By varying the field of the electromagnet, it was possible to move the sensitive spot in the depth direction giving a depth resolution of ~2 mm over a limited region.

The approaches mentioned above can be broadly grouped into two categories: coarse and fine resolution. The second category, explored by Refs. [8,9,11], represents the UMR equivalent of stray field imaging (STRAFI) [2,13], in which a strong gradient is used to obtain micron resolution profiles of samples with short relaxation times. In a Fourier transform STRAFI experiment, the thickness of the imaging volume in the depth direction is necessarily traded off against resolution. To overcome this difficulty, the sample is often displaced relative to the magnetic field, as in Ref. [8], in order to give greater spatial extent to the measurement. While the approach of Ref. [9] is more convenient, the resolution is limited by the curvature of the field. Consequently, the high gradient merely limits the maximum extent of the sample, but does not yield exceptional spatial resolution. For a UMR measurement in which resolution <10 μm is required, Perlo's approach [8] appears to be the best option.

In a regime where lower resolution (~100 μm) is necessary, such as profiling of thicker coatings or layers, acceptable resolution may be obtained over a larger region without moving the sample or magnet, by reducing the gradient strength. To this end, a unilateral sensor has been developed with a constant gradient of +30 G/cm over a range of ~8 mm. The instrument consists of a single magnet, topped with a shaped pole piece made from high permeability iron. This configuration was designed using the scalar potential method [14,15], through which the magnet size and pole piece shape were synthesized based on the desired B_0. Because of the moderate gradient, the desired sample bandwidth can be excited using a suitably short hard pulse at a single center frequency, or a series of soft pulses. As a result, displacing the magnet with respect to the sample is not required with this approach. Profiles are obtained through a spin-echo experiment, and require no gradient coils or RF switching hardware. The field curvature limits the resolution to 100's of μm, suitable for a variety of near-surface profiling applications.

2. Theory–Scalar potential design

A detailed description of the scalar potential design technique for UMR can be found in Ref. [15]. The design takes place in the two-dimensional ZY plane using the conventions in that reference. The idea is to specify a magnetic field B_0, and synthesize its associated scalar potential $\phi(z,y)$. High permeability material shaped according to one or more contours of this potential can then be placed on a magnet array in order to give the desired field. The material is shaped in two dimensions, and extended in the third in order to remove end effects. A magnetic field can be defined through $B = \nabla\phi$ with $\phi(z,y)$ satisfying

$$\nabla^2\phi = 0. \tag{1}$$

A solution to Eq. (1) is

$$\phi = \sum_{n=1}^{N} c_n e^{-nay}\cos(naz), \tag{2}$$

which describes a potential evenly symmetric about the z-origin, and periodic in z with period $2\pi/a$. Taking the gradient of Eq. (2) gives an expression for a magnetic field in terms of the arbitrary constants a and c_n. In previous work [15], these constants were numerically optimized to give a specified field. Here, by considering the field and its derivatives at a single point in space, it is possible to analytically solve for the required constants. This simplified condition can serve as a starting point for more complex optimizations but was found here to be sufficient. More rigorous control over the field characteristics can be achieved, for example, by including the lateral variation in the field in the optimization. However, as will be discussed, the approximations used in synthesizing the magnet array using this method will lead to discrepancies between the field that is specified and that which is achieved. For this reason, it is in general not appropriate to over specify the field profile. These considerations will be the topic of an upcoming publication.

To define a field B_0, with constant gradient at a given point over the center of the array $(z,y) = (0,d)$, a minimum of three parameters should be specified: the field strength at the point, the field gradient at the point, and the second spatial derivative of the field, ensuring that the gradient is constant to second order. These constraints can be summarized as

$$\begin{aligned} |B_0(0,d)| &= B \\ \left.\frac{\partial|B_0|}{\partial y}\right|_{(0,d)} &= G \\ \left.\frac{\partial^2|B_0|}{\partial y^2}\right|_{(0,d)} &= 0. \end{aligned} \tag{3}$$

Higher derivatives could be set to zero to give a more constant gradient. However, we have found that the constraints in Eq. (3) lead to a reasonable compromise between gradient uniformity and design complexity. The gradient of Eq. (2) is

$$B_0 = \sum_{n=1}^{N} nac_n e^{-nay}(-\sin(naz)\hat{z} - \cos(naz)\hat{y}) \tag{4}$$

so

$$|B_0(0,y)| = \sum_{n=1}^{N} nac_n e^{-nay}. \tag{5}$$

Fixing a, and choosing N=3 to enforce the constraints in Eq. (3) gives a linear system of three equations and three unknowns which can be solved by matrix inversion for

the c_n parameters. A contour of the scalar potential defined in Eq. (2) can now be selected to define the shape of a pole piece giving the desired field characteristics. The parameter a defines the approximate width of the magnet. Because the actual value of B will depend on the strength of the magnets used in the array construction, it is convenient to normalize the field strength to unity. The gradient will scale with the field and can thus be expressed as a percentage of the field strength.

Because the scalar potential described in Eq. (2) is evenly symmetric, the magnetic field will be principally normal to the plane of the magnets. While, this configuration requires special RF coil designs to produce an orthogonal B_1, experience has shown that for a unilateral magnet designed using the scalar potential formulation, a constant gradient design with B_0 in this direction is much more easily realized than with B_0 parallel to the array. Furthermore, in this case the formulation results in a class of instrument comprised of single magnets topped with single pole pieces, simplifying construction.

The desired magnetic field is generated by selecting one or more contours of scalar potential described by the optimized parameters to define the shape of pole pieces sitting atop permanent magnets. In practice, the periodic function $\phi(z,y)$ is truncated to within one period. We have found that for magnets designed with the constraints given in Eq. (3), a wide range of gradient values will give a scalar potential function with contours that are continuous over the majority of a period. Consequently, the potential can be realized with a single pole piece. The shape of this piece is generated by defining lines $y = y_0$ for the bottom of the pole and $y = y_1$ for the top. This second line is selected such that the surface of the pole piece is below the desired sensitive volume, while the first is chosen here to be $y = 0$ for convenience. The value ϕ_c of the selected contour is determined as

$$\phi_c = \max \phi(z, y_1). \tag{6}$$

From Eq. (2), the contour is then defined by

$$\sum_{n=1}^{3} c_n R^n \cos(naz) - \phi_c = 0, \tag{7}$$

with $R = e^{-ay}$. Eq. (7) is a polynomial with roots $R_i(z)$ from which the contour shape can be determined as

$$y(z) = -\frac{\ln(R_i(z))}{a}, \tag{8}$$

where care must be taken such that the root corresponding to the location within the real potential field is selected.

3. Sensor design

3.1. Magnet array

Using the design procedure discussed in Section 2, a pole piece was synthesized to give a field which increased with distance from the magnet with a gradient equal to 1.3% of the field strength (this gives 25 G/cm at 8 MHz). For this design, it was desired that the sensitive volume be immediately above the face of the pole piece, and therefore a scalar potential contour with maxima at $y_1 = 2.17$ cm was selected to form the pole.

The pole piece was machined from iron using a 3-axis ES-V4020 CNC vertical machining center. A single NdFeB magnet 13.9 cm square and 5 cm thick purchased from Yuxiang Magnetic Materials Ind. Co., Ltd, with a remanence specified by the manufacturer of 1.3 T, was positioned below the pole piece to generate the static field. The magnet was enclosed in an aluminum box with a 1.25 cm thick iron plate at the bottom. The purpose of the iron plate is to increase the field strength above the magnet and limit the stray field below it. Experience indicates that this plate will not affect the shape of the field. The total weight of the system is just under 14 kg. A photograph of the completed magnet assembly is given in Fig. 1. Fortuitously, the contour defining the pole piece has a depression near the center, allowing an RF resonator to be positioned below the sensitive volume.

To verify the design, the magnetic field above the assembly was simulated using commercial software (Vector Fields, Aurora, IL3-axis) and measured using a Hall sensor (Lakeshore, Westerville, OH) and 3-axis computer controlled positioning system (Velmex, Bloomfield, NY). The iron plate on the bottom of the magnet was not modeled. Rather, the remanence of the NdFeB magnet modeled in the simulation was adjusted until the field strength agreed with that measured. This occurred for a simulated remanence of 1.2 T which is below that specified for the magnets but within manufacturing tolerances. Fig. 2(a) shows the simulated magnetic field in the zy plane over the center of the magnet with the pole piece shape superimposed. Fig. 2(b) illustrates the field calculated according to Eq. (4) while Figs. 2(c) and (d) present contour plots of the simulated and measured magnetic field magnitude. The plots

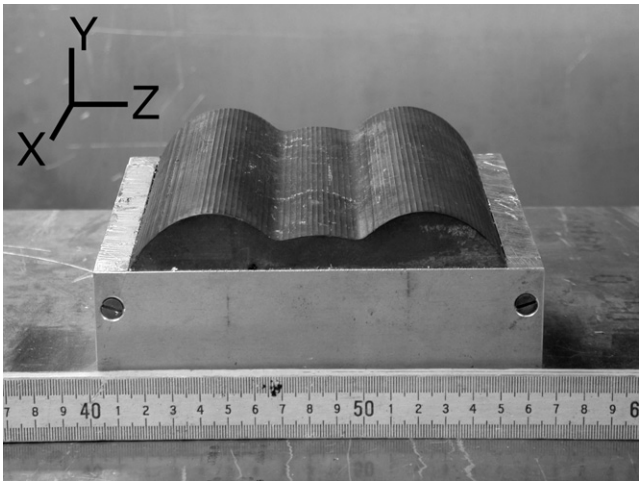

Fig. 1. Photograph of the magnet with length scale included. The iron pole piece sits atop a 13.9 cm square NdFeB magnet 5 cm thick. The magnet is housed in an box with aluminum sides and a steel bottom 1.25 cm thick.

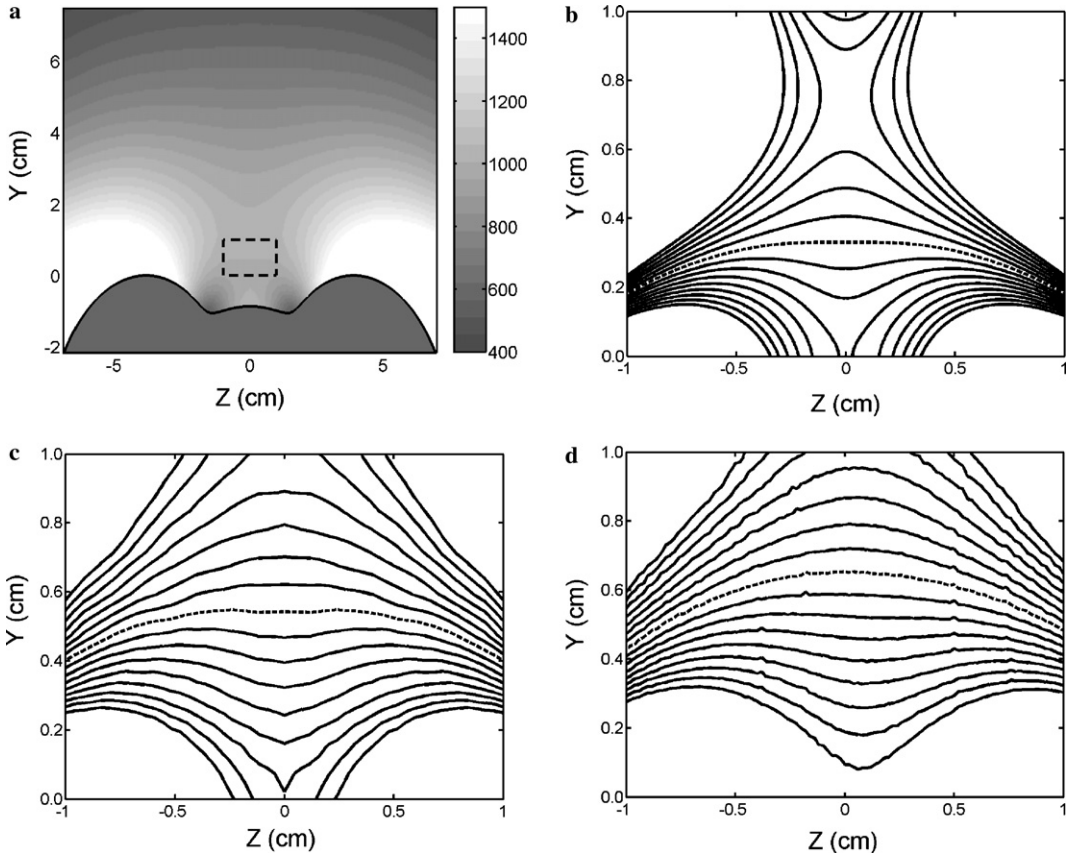

Fig. 2. (a) Contour plot of the simulated magnetic field, showing the shape of the pole piece and the region of interest. The color scale indicates the field strength in Gauss. (b) Field contours calculated according to Eq. (4) assuming a magnet array of infinite extent. (c) Simulated magnetic field in the region 2 cm wide centered 0.5 cm above the face of the magnet. (d) Measured magnetic field in the region 2 cm wide centered 0.5 cm above the face of the magnet. In (b), (c) and (d), the dashed line indicates $B_0 = 1006$ G. The contours are at 2 G intervals in (c) and (d) and at 1 G intervals in (b). The field in plot (b) has been scaled uniformly to correspond to the measured field strength.

are for the region around the sensitive spot highlighted in Fig. 2(a). In these plots, $y = 0$ represents the upper face of the pole piece. The constant contour spacing up the center of these plots at $z = 0$, indicates a constant gradient in this region. The field exhibits different degrees of curvature with increasing z and is flattest just below $y = 0.6$ cm in the measured plot (d). With the permanent magnet employed, the field strength is just above 1000 G in the center of this region. Significant disagreement is noted between the actual field and that specified by the design. While the central areas of the sensitive spot are qualitatively similar, the region in which the contours are flattest is offset by $\sim$2 mm between plots (b) and (d). Furthermore, the gradient is larger than specified. Fig. 3 shows the measured field at $z = 0$ as a function of distance from the magnet. The field increases linearly over a region just over 0.6 cm thick, remaining reasonably linear over almost 1 cm, and eventually reaches a maximum then decays. A least squares fit in the linear region gives a gradient of 30.9 G/cm or 3.1% of the field strength. This differs from the design value by more than a factor of 2. The differences between the calculated and simulated/measured field profiles are due to the design assumption that the scalar potential and field are periodic in z while they have clearly been truncated in manufacturing the magnet. The agreement between the simulated and measured results indicates that errors due to manufacturing tolerances are insignificant in this case. Nevertheless, the linearity of the field variation is preserved, and the measured gradient value is close to that which was desired,

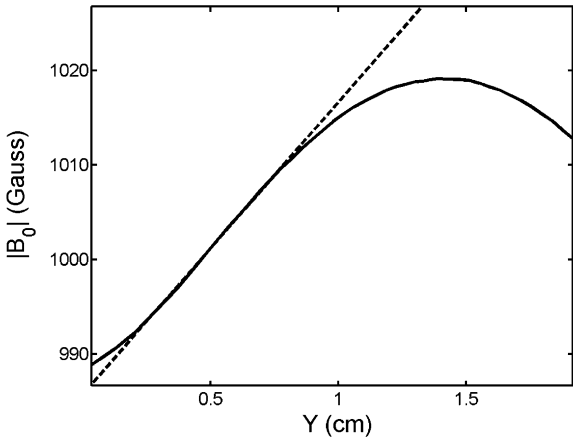

Fig. 3. Measured field profile at $z = 0$ through the sensitive volume (solid line). A least squares fit to the linear region (dashed line) gives a gradient of 30.9 G/cm.

albeit at a lower field. In this design, the variation has the positive effect of enlarging the sensitive spot, both in terms of the extent of the linear region and the flatness of the field.

The gradient value was also verified using steady gradient stimulated echo (SGSTE) diffusion measurements [16,17] of diffusive attenuation in water. Ignoring relaxation, the diffusive attenuation for this sequence is given by

$$\ln\left(\frac{I}{I_0}\right) = -\gamma^2 G^2 D \tau_1^2 \left(\tau_2 + \frac{2}{3}\tau_1\right),$$

where τ_1 and τ_2 are the diffusion times as defined in [16], I is the echo intensity, I_0 is the echo intensity for very short diffusion times, G is the gradient, γ is the proton gyromagnetic ratio, and D is the diffusion coefficient. Measurements were made with the resonator described in the next section on a 1 cm square bottle of distilled water 4.5 cm long with its bottom at the pole surface, for different diffusion times. The attenuation is plotted against the factor $\tau_1^2(\tau_2 + (2/3)\tau_1)$ in Fig. 4. Using a diffusion coefficient for water of $2.02 \times 10^{-9}\mathrm{m}^2/\mathrm{s}$, the gradient value calculated from the slope of this line is 39.1 G/cm. This slightly larger value is expected due to the field curvature away from the z-origin. Fig. 2(c) shows more closely spaced contour lines in this region, indicating a higher gradient. Nevertheless, the linearity of the diffusive attenuation over a large range of diffusion times indicates that the assumption of a constant gradient is reasonable.

3.2. Resonator

Because B_0 is principally orthogonal to the plane of the magnet, a surface coil generating a B_1 field directed parallel to its plane must be employed for truly unilateral measurements. To this end, a 'double D' coil similar to those in Refs. [18,19] was used. The coil consists of two counter-wound semi-circle shaped loops situated immediately adjacent to one another such that the B_1 field curls between then and is therefore parallel to the plane of the coil over its center. Each loop had 4 turns, and the coil was 3 cm in diameter. The effective sensitive volume defined by the coil is limited to a central region, as the current return paths comprise the coil's outer portion. This type of coil does, however, generate a spurious B_1 field around the return wires which was not compensated for in this work. The coil was matched capacitively to a frequency variable between 4.23 and 4.27 MHz.

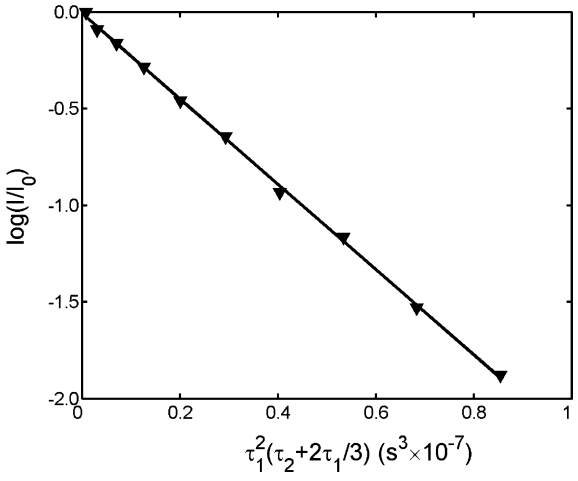

Fig. 4. Plot of diffusive attenuation for distilled water measured using the SGSTE diffusion sequence. The measured data points (triangles), when fit with a least squares procedure (solid line), give a gradient of 39.1 G/cm in the sensitive spot. Imaging parameters were: 32 scans, 5 s delay between scans, 1024 echoes averaged after the SGSTE sequence [16] with an echo time of 150 μs. The total measurement time was under 3 minutes per data point.

4. MRI profiling

To investigate the resolution available from the field within the sensitive volume, several MRI profiling experiments were carried out. The moderate field gradient allows spins within the sensitive volume to be simultaneously excited using a broadband RF pulse. As a result, spin density profiles from within the sensitive volume can be obtained by Fourier transformation of the echo acquired from a standard 90 °-τ−180° spin echo experiment.

Because of the curvature revealed in the field magnitude plot Fig. 2(d), the resolution of a y-directed profile will vary with y. This phenomenon was investigated by imaging the edge of a 1 cm rubber cube phantom. The sample size was selected to only be excited by the central lobe of the B_1 field. The theoretical profile of this sample would be a step function. In regions where the field is reasonably flat over the extent of this sample, i.e., between $y = 5$ mm and $y = 6$ mm, the resolution should be higher than that available above and below this spot. Examining profiles with the bottom of the cube at varying y gives a direct measure of the blurring present in an image. Fig. 5 shows profiles of this sample at (a) $y = 1$ mm, (b) $y = 3$ mm, (c) $y = 6$ mm and (d) $y = 8$ mm from the surface of the pole. All profiles experience a roll-off in intensity at larger y due to the limited extent of B_1. As expected, at 1 mm from the surface, the resolution is quite poor, and the step is spread over almost 2 mm. In this case, the resolution loss is a combination of field curvature and the weaker gradient present close to the pole surface. The situation improves dramatically at 3 mm, and at 6 mm, the step occurs within one pixel (~150 μm), indicating a maximally flat field. At 8 mm, the resolution worsens again, but is likely made better since at larger distances from the coil, the excited spins are principally those close to the coil axis ($z = 0$). These results show that it is possible to obtain profiles with resolutions on the order of 100 μm. The challenge lies in generating a RF field that is selective enough in the x and z directions to maximize resolution, and which has a large enough extent in y to excite the entire imaging volume.

To demonstrate imaging of a layered sample, a phantom was made comprising three layers of rubber, 1 cm by 1 cm square and 1 mm thick, separated by glass slides 1 mm in thickness. The resulting profile is shown in Fig. 6. All three

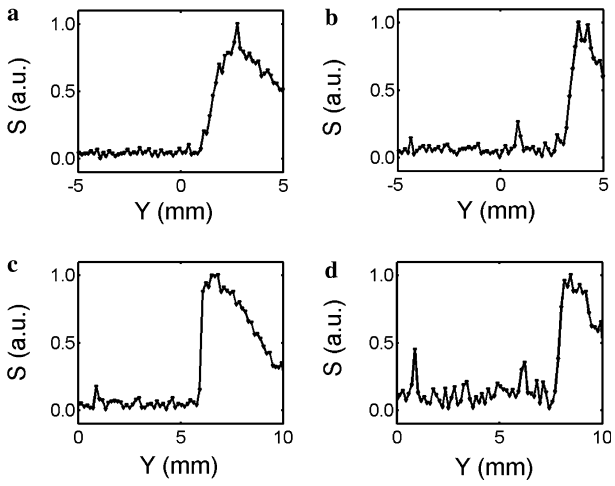

Fig. 5. MRI profiles of the edge of a rubber phantom showing the position-dependent resolution of the magnet. Scale indicates distance from the top of the pole in the y-direction. The edge of the phantom was positioned (a) 1 mm, (b) 3 mm, (c) 6 mm and (d) 8 mm from the pole surface. The position scale in the images was calculated assuming a gradient of 30.9 G/cm. Profiles (a) and (b) were collected with a surface coil positioned below the pole surface. For (c) and (d), the probe was repositioned such that its surface was 3 mm above the pole face to improve SNR. The profiles were obtained by Fourier transformation of the spin echo. Imaging parameters were: 4096 scans, an echo time of 0.612 ms, delay between scans of 100 ms, acquisition window 512 us with a dwell time of 1 μs, 180° pulse width of 7 μs with a 90° pulse achieved by halving the pulse power.

peaks and the spacing between them are readily observed. The signal from the third slice is substantially reduced compared to the first two due to B_1 effects. This problem could be solved either by normalizing the profile according to the known roll-off of B_1 or by adjusting the pulse width and frequency to better excite this area.

The spatial resolution of Fig. 6 is less than that of the profiles of Fig. 5. We attribute this to sample surface roughness and imprecise sample leveling. While undesirable, this resolution loss illustrates that in many realistic samples, a theoretical spatial resolution better than 0.5 mm will not be realized in experiment to intrinsic sample non-ideality.

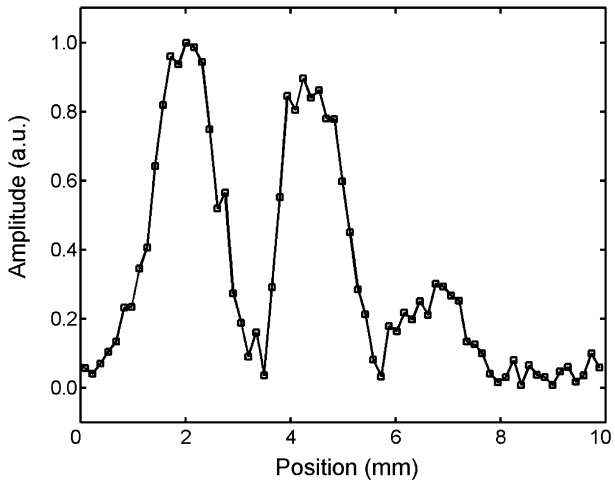

Fig. 6. MRI profile of a phantom sample consisting of three 1 cm square slices of rubber 1 mm thick, with a 1 mm separation. The three slices are easily resolved, with increased blurring occurring near the face of the magnet and lower signal away from the coil. The phantom was positioned 1 mm from the pole surface. Experimental parameters were the same as those used for the plots in Fig. 5.

5. Conclusions

The design and construction of a magnet assembly producing a magnetic field with linear spatial variation in one direction has been presented. The field gradient allows 1D MRI profiling using a simple spin-echo experiment. The profile resolution is limited by the field curvature. The maximum resolution achievable is below 150 μm but is dependent on the extent of the sample being investigated as well as the resonator design. The marked advantage of this system compared to other unilateral profiling hardware is the larger sensitive spot thickness. This permits coarse resolution imaging of thicker layers without requiring that the magnet be displaced relative to the sample.

The constant gradient may also find relevance in diffusion measurements. As indicated by the high quality plot of diffusive attenuation in Fig. 4, the magnetic field produced by this assembly has a strong potential for this application.

The magnetic field was designed using a scalar potential approach through which the pole piece shape was tailored to produce the desired field. This method may be used to design and manufacture magnet assemblies with specific gradient values. Measurements have shown that while the field is in keeping with the design, there is a significant discrepancy between the analytically determined gradient and its actual value. The magnet array is also inefficient in that a large (13.9 cm width) array is required to produce a small (<1 cm width) sensitive volume. The discrepancy in gradient values, along with the inefficiency, are both the result of the magnet assembly being a finite approximation of an infinite structure. Future work, will address this approximation in order to facilitate better designed magnet arrays.

Acknowledgments

A.E.M. thanks NSERC for financial assistance (CGS D). B.J.B. and I.V.M. thank NSERC for Discovery grants. I.V.M. and B.J.B. thank NSERC for an I2I grant. B.J.B. thanks the Canada Chairs program for a Research Chair in MRI of materials (2002–2009). The UNB MRI Centre is supported by an NSERC Major Facilities Access Award. We thank Rod MacGregor for technical assistance and Trevor Desroches, Murray Olive, and Brian Titus for manufacturing the pole piece and magnet assembly.

References

[1] R.L. Kleinberg, A. Sezginer, D.D. Griffin, M. Fukuhara, Novel NMR apparatus for investigating an external sample, J. Magn. Res. 97 (1992) 466–485.

[2] J. Mitchell, P. Blümler, P.J. McDonald, Spatially resolved nuclear magnetic resonance studies of planar samples, Prog. Nucl. Magn. Reson. Spectrosc. 48 (2006) 161–181.
[3] G. Eidmann, R. Savelsberg, P. Blümler, B. Blümich, The NMR MOUSE, a mobile universal surface explorer, J. Magn. Res. A 122 (1996) 104–109.
[4] B. Blümich, V. Anferov, S. Anferova, M. Klein, R. Fechete, M. Adams, F. Casanova, Simple NMR-mouse with a bar magnet, Conc. Magn. Reson. B 15 (2002) 255–261.
[5] S. Rahmatallah, Y. Li, H.C. Seton, I.S. Gregory, R.M. Aspden, Measurement of relaxation times in foodstuffs using a one-sided portable magnetic resonance probe, Eur. Food Res. Technol. 222 (2006) 298–301.
[6] P.J. Prado, Single-sided imaging sensor, Magn. Res. Imaging. 21 (2003) 397–400.
[7] J. Perlo, F. Casanova, B. Blümich, 3D imaging with a single-sided sensor: an open tomograph, J. Magn. Res. 166 (2004) 228–235.
[8] J. Perlo, F. Casanova, B. Blümich, Profiles with microscopic resolution by single-sided NMR, J. Magn. Res. 176 (2005) 64–70.
[9] S. Rahmatallah, Y. Li, H.C. Seton, I.S. Mackenzie, J.S. Gregory, R.M. Aspden, NMR detection and one-dimensional imaging using the inhomogeneous field of a portable single-sided magnet, J. Magn. Res. 173 (2005) 23–28.
[10] US Patent 6,489,872. E. Fukushima, J.A. Jackson, Unilateral magnet having a remote uniform field region for nuclear magnetic resonance.
[11] W.-H. Chang, J.-H. Chen, and L.-P. Hwang, Single-sided mobile NMR with a Halbach magnet, Magn. Reson. Imag. In press.
[12] M.C.A. Brown, D.A. Verganelakis, M.J.D. Mallett, J. Mitchell, P. Blümler, Surface normal imaging with a hand-held NMR device, J. Magn. Res. 169 (2004) 308–312.
[13] P.J. McDonald, Stray field magnetic resonance imaging, Prog. Nucl. Magn. Reson. Spectrosc. 30 (1997) 69–99.
[14] P.M. Glover, P.S. Aptaker, J.R. Bowler, E. Ciampi, P.J. McDonald, A novel high-gradient permanent magnet for the profiling of planar films and coatings, J. Magn. Res. 139 (1999) 90–97.
[15] A.E. Marble, I.V. Mastikhin, B.G. Colpitts, B.J. Balcom, An analytical methodology for magnetic field control in unilateral NMR, J. Magn. Res. 174 (2005) 78–87.
[16] R. Kimmich, NMR Tomography, Diffusometry, Relaxometry, Springer, Berlin, 1997, pp. 180–181.
[17] D.G. Rata, F. Casanova, J. Perlo, D.E. Demco, B. Blümich, Self-diffusion measurements by a mobile single-sided NMR sensor with improved magnetic field gradient, J. Magn. Res 180 (2006) 229–235.
[18] S. Utsuzawa, R. Kemmer, and Y. Nakashima, Unilateral NMR system by using a novel barrel shaped magnet, Proceedings of the 5th Colloquium on Mobile NMR, Sept 21-23, 2005, Perugia, Italy.
[19] S. Anferova, V. Anferov, D.G. Rata, B. Blümich, J. Arnold, C. Clauser, P. Blümler, H. Raich, A mobile NMR device for measurements of porosity and pore size distributions of drilled core samples, Conc. Magn. Reson. B 23 (2004) 26–32.